Fatigue Analysis of Materials and Structures Using a Continuum Damage Model

O. Salomón -- S. Oller -- E. Oñate

International Center for Numerical Methods in Engineering (CIMNE) and Universitat Politècnica de Catalunya, E.T.S. Ingenieros de Caminos, Canales y Puertos, C/Gran Capitán S/N, Modulo C1, Campus Nord UPC, 08034 Barcelona, Spain
salomon@cimne.upc.es
oller@cimne.upc.es
onate@cimne.upc.es

ABSTRACT: The scatter in the fatigue life of the metallic structures seems to be mainly caused by internal defects of the material (porosity, inclusions as oxide films and carbon layers, grain boundaries, etc.). As discontinuities in geometry, defects cause stress concentration and are therefore prone to fatigue crack initiation. Here, a fatigue model based in continuum mechanic with its general expressions for the elasto-plastic-damage constitutive equations, previously developed by the authors, is extended to include the effects of material internal defects. In this stress life approach the material is considered to be non-homogenous. The material strength is randomly assigned and Stress-N° of cycles curves are scaled down according to material strength of each point. Limit values for material strength are based on experimental tests of samples with different degree of porosity.

RÉSUMÉ: La dispersion dans la vie des structures métalliques, du point de vue de la fatigue, semble être causé principalement par défauts internes de la matière (porosité, inclusions telles que films d'oxyde et couches de carbone, etc.). De même que les discontinuités dans la géométrie, les défauts sont la cause d'une concentration de tensions et par conséquent, cause de l'initiation de la fissure pour fatigue. Dans ce travail, un modèle de la fatigue basé sur la mécanique des milieux continus avec ses expressions générales pour les équations constitutives de dommage elasto-plastique, précédemment développées par les auteurs, est étendu afin d'inclure les effets des défauts internes de la matière. Dans cette approche au tensions, la matière est considérée comme non-homogène. La résistance matérielle est assignée au forme aléatoire et des courbes tension-N° de cycles sont ajustées en fonction de la résistance matérielle en chaque point. Les valeurs limites pour la résistance matérielle sont basées sur des tests expérimentaux de spécimens ayant différents degré de porosité.

KEY WORDS: Internal defect, Life prediction, Damage mechanics

MOTS-CLÉS: défauts internes, prédiction de la vie a fatigue, mécaniques du dommage

Published at *International Journal of Forming Processes*, Vol. 5 Nos. 2-3-4, pp 493-503, 2002

1. Introduction

Fatigue can be defined as the process of permanent, progressive and localised structural change which occurs to a material point subjected to strains and stresses of variable amplitudes which produces cracks leading to total failure after a certain number of cycles. A progressive loss of the material strength occurs as a function of the number of stress/strain cycles, reversion index, load amplitude, etc. Loss of strength may be interpreted as micro-cracking followed by crack coalescence leading to the final collapse of structural parts. Failure typically takes place for stress levels well below the strength limit of the material obtained in static tests.

Structural materials are, in general and at less from a microscopic point of view, non-homogeneous materials. In the case of metals, they include discontinuities such as grain boundaries, microscopic pores, and other particles as impurities and carbon. All of them are commonly considered as defects. This does not denote that those materials are defective and consequently useless. Defects are a normal feature of metallic material microstructure. However, defects are also source of local stress concentrations inducing local plasticity and/or damage and therefore they can turn into fatigue crack initiation sites.

According to their location, defects can be classified as internal or external. External or surface defects can be introduced through component assembly, impact of foreign objects or material processing. They can be detectable by optical inspection. Internal defects, in contrast, are introduced in the structure during manufacturing. The precise size, location and type of defects cannot be predicted. Only post-manufacturing inspections (i.e.: radiography and computed tomography) can provide accurate information about the defect population present in structures.

Internal defects in metals include porosity, inclusions as oxide films or carbon layers and, in case of welded parts, lack of fusion and lack of penetration of the welded joint. As discontinuities in geometry, defects cause stress concentration and are therefore prone to fatigue crack initiation.

The classical and simplest approach to take into account the effects of internal defects on the fatigue strength of structures has been to consider the fatigue stress limit of the material reduced by a size factor. The larger the size of a part, the more chance there is for internal defects to be present.

This paper extends the previous work of the authors (Oller *et al.*,01; Salomón *et al.*, 02, 99), on the application of the theoretical framework of continuum mechanics to the study of non linear fatigue problems, accounting for the influence of internal defects in the resulting fatigue prediction model. As in previous work, restriction is made here to small deformations and isotropic damage.

2. Internal Defects in Metallic Structures

From a detailed study (DARCAST, 00) conducted on aluminium alloy samples, AlSi8.5Cu3.5Fe, at last two basic conclusions arise on the influence of internal defects:

- Porosity significantly lowers the static properties of the material (strength and strain to failure).
- The reduction is almost linear with the porosity level (classified as A0, A2 and A4 according to ASTM E505 standard)

A significant reduction in the fatigue strength was also found when the degree of porosity was increased from A0 to A2. The decrease was distinctly lower from A2 to A4. The ratio fatigue-strength/static-strength was 0.54, 0.44 and 0.51 for materials A0, A2 and A4, respectively. As fatigue data suffer of large scattering this observation is not conclusive.

A real industrial component, an alternator support made of the same material, was also experimentally tested and numerically analysed. The alternator support was selected among the components of the supplier actual production. Two batches were provided (about 50 components) for the experimental testing: one batch of non-porous components (components with an acceptable level of porosity) and one batch of porous components; the distinction being made by the supplier based on radioscopy examination. Subsequent laboratory examination showed that a scattered porosity was also present in the non-porous components.

The fatigue testing showed that for both components (porous and non-porous) four different regions of failure could be identified. At regions of failure not highly stressed, pores of significant dimensions, oxide films and defects in the microstructure were observed on the fracture surfaces. The difference in the fatigue limit, as found for the porous and non-porous components, was observed to be statistically non significant.

Numerical simulations of the aluminium support were done and results of the analysis were compared with those from experimental testing. Figure 1 compares experimental regions of failure with stress distribution obtained from the numerical simulation. Regions of failure 2, 3 and 4 are in coincidence with extended highly stressed areas. Figure 1 also displays the correlation between the damage areas due to fatigue and experimental regions of failure. Damage is observed in concordance with regions of failure 3 and 4. Region of failure 2 (upper part) correspond to a highly compressed area what dismiss the fatigue effects. For region of failure 1 the numerical analysis only yielded a small area of stress concentration due to local geometry conditions.

Life prediction of the aluminium support based on numerical analyses (material A2) agreed with experimental tests: Failure around 900.000 cycles for a maximum load of 10.5 kN (50% probability of survival, porous and non-porous components.

Non-porous components indicate acceptable level of porosity). A different material characterization (as A0 or A4) in the analysis would bring a different lifespan, but the region where failure occurs would always be the same if the material is considerer homogeneous.

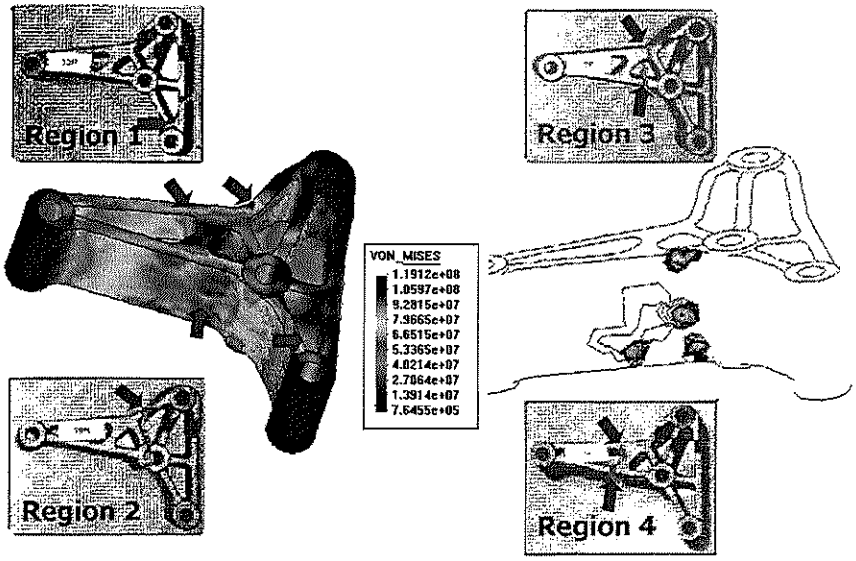

Figure 1. Stress and fatigue damage distribution from numerical simulation and experimental regions of failure.

Internal defects, mainly porosity, can be regarded as responsible for the fatigue failure of the component at four different regions. Therefore, a first approach to simulate this behaviour is to consider a random distribution of such defects. As it was mentioned before, porosity reduces, in an almost linear way, the static material strength. Consequently, the value of material strength is randomly assigned, material is not homogenous any more. Maximum and minimum values will be the material strength experimentally obtained for samples with porosities A0 and A4, respectively.

Concerning fatigue characterization of the material, porosity not only causes a reduction in the fatigue strength, but eventually also a change in the slope of the Stress-N° of cycles curves. In this paper a master S-N curve is proposed, based in experimental results on rotating bending fatigue, for the whole structure to be analysed. That master curve is scaled down according to the randomly assigned material strength of each point.

3. Fatigue Analysis using Continuum Mechanics

The theoretical structure of continuum mechanics is suitable for the study of non-linear fatigue problems (Osgood, 82; Suresh, 98). In previous works of the authors (Oller *et al.*,01; Salomón *et al.*, 02, 99) a deterministic fatigue prediction model based on a continuum mechanics formulation, considering coupling between elasticity, damage and plasticity, was developed.

The formulation assumes that each point of the solid follows a damage-elasto-plastic constitutive law with the stress (S) evolution depending on the free elastic strain variable (E^e) and a set of internal plastic and damage variables $q=\{\alpha^p,d\}=\{E^p, \kappa^p,d=\kappa^d\}$, were E^p and $\kappa^{ini}\leq(\kappa=\kappa^p+\kappa^d)\leq 1$ represent the plastic part of the strain and a unit normalized dissipation composed by the plastic plus damage parts, respectively. The initial defect level defines the initial threshold of the normalized dissipation $\kappa^{ini}=d^{ini}$ in the initial damage form. The free energy for isothermal, isentropic and adiabatic processes and for small elastic strains and large plastic strains is written in the reference configuration, accepting the additivity of its elastic Ψ^e and plastic Ψ^p parts, as

$$\Psi=\Psi^e(E^e_{ij},d)+\Psi^p(\alpha^p_i)=(1-d)\frac{1}{2m^o}\left[E^e_{ij}\,C^o_{ijkl}\,E^e_{kl}\right]+\Psi^p(\alpha^p_i) \quad (1)$$

where E^e is elastic Green strain tensor, m^0 is the material density, $d=\kappa^d$ is the internal mechanical damage variable for the damage processes $d^{ini}\leq\left(d=\kappa^d\right)\leq 1$ with the initial value $d^{ini}\equiv\kappa^{ini}$ provided by the defect level, and C^0_{ijkl} the initial constitutive tensor. The stress tensor in the reference configuration S_{ij} can be expressed as

$$S_{ij}=m^o\frac{\partial\Psi}{\partial E^e_{ij}}=(1-d)\,C^o_{ijkl}\,E^e_{kl} \quad (2)$$

For the plastic behaviour, the general forms of the yield F and potential G plastic functions take into account the influence of the current stress state, the internal plastic variables, and other variables such as the number of cycles N:

$$\begin{aligned} &F(S_{ij},\kappa,\theta)=f(S_{ij})-K(S_{ij},\kappa,N)\\ &G(S_{ij})=g(S_{ij})=\text{constant.}\end{aligned} \quad (3)$$

where $f(S_{ij})$ and $g(S_{ij})$ are the uniaxial equivalent stress functions, $K(S_{ij},\kappa,N)$ is the strength threshold (see Figure 2). All the internal variables at

current time t are obtained by means of an integration process $\alpha_i^p = \int_0 \dot{\alpha}_i^p dt$, starting from its evolution law $\alpha_i^p = \dot{\lambda} H_i^p(S_{kl}, \alpha_k^p)$, where λ is the plastic consistent factor.

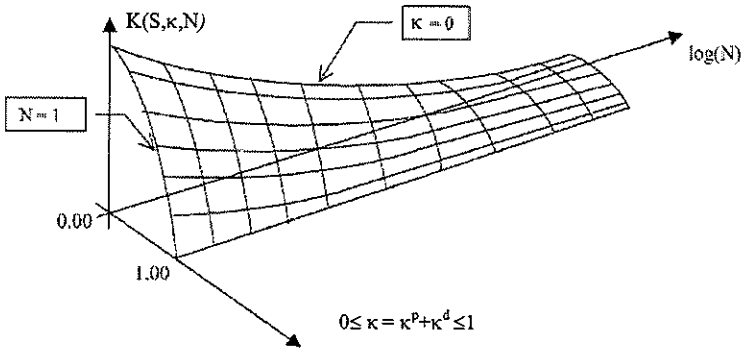

Figure 2. Uniaxial strength threshold for a symbolic material.

The damage function is defined as

$$G^D(S_{ij}, \kappa, \theta) = \bar{S}(S_{ij}) - K(S_{ij}, \kappa, N) \tag{4}$$

where $\bar{S}(S_{ij})$ is the uniaxial equivalent stress function in the undamaged space, $K(S_{ij}, \kappa, N)$ is the same strength threshold as in (3) and $\kappa^d = d = \int_0 \dot{d}\, dt$ the damage internal variable with an evolution defined as $d = \dot{\mu} H^D(S_{kl}, d)$, where μ is the consistency damage factor. In both, (3) and (4), the normalized dissipation is defined as $\kappa = \kappa^p + \kappa^d = \left(\Xi^p + \Xi^d\right)/\Xi^{\max}$, where Ξ^p, Ξ^d, $\Xi^{\max}$ are the Clausius-Duhem dissipation for the current plastic, damage process and its maximum capacity of the solid dissipation at each point, respectively.

The effect of the number of cycles on the plastic and/or damage consistency conditions ($\dot{F} = 0$, $\dot{G}^D = 0$) is introduced as follows,

$$f(S_{ij}) - \underbrace{K(S_{ij}, \kappa).f_{red}(N, S_{med}, R)}_{K(S_{ij}, R, N)} = 0 \tag{5}$$

$$\bar{S}(S_{ij}) - \underbrace{K(S_{ij}, \kappa).f_{red}(N, S_{med}, R)}_{K(S_{ij}, R, N)} = 0 \tag{6}$$

where $0 \le f_{red} \le 1$ represent the unit normalized reduction part of the strength threshold K —plastic and/or damage strength evolution— by load cyclic effect

4. *S-N* Curves

Stress-N° of cycles (*S-N*) curves are experimentally obtained by subjecting identical smooth specimens to cyclic harmonic stresses and establishing their life span measured in number of cycles. The curves depend on the level of the maximum applied stress and on the ratio between the lowest and the highest stresses ($R = S_{\min} / S_{\max}$). In previous works (Oller *et al.*,01; Salomón *et al.*, 02) an exponential function to approach steel and aluminium experimental *S-N* curves was proposed. This function depends on and is capable of dealing with any value of the ratio between minimum and maximum stress. However, it is a bit difficult to adjust its parameters to obtain a good approximation to experimental curves, which are usually not defined over the whole life-span of the material. Instead of using such an exponential function, here the experimental data is introduced by points in a table-like mode.

Usually, *S-N* curves are obtained for a fully reversed stress state ($R = S_{\min} / S_{\max} = -1$) by rotating bending fatigue tests. This zero mean stress is however not typical of real industrial components working under cyclic loads. Based on the actual value of the *R* ratio and a basic value of the endurance stress *Se* (for *R* = *-1*) the model proposed postulates a threshold stress S_{th}. The meaning of S_{th} is that of an endurance stress limit for a given value of $R = S_{\min} / S_{\max}$; if the actual value of *R* is *R*= -1 then, $S_{th} = S_e$.

$$\begin{aligned} S_{th} &= S_e + (S_u - S_e) \cdot (0.5 + 0.5 \cdot R)^{STHR1} \longrightarrow abs(R) \le 1 \\ S_{th} &= S_e + (S_u - S_e) \cdot (0.5 + 0.5 / R)^{STHR2} \longrightarrow abs(R) \ge 1 \end{aligned} \tag{7}$$

STHR1 and *STHR2* are material parameters that need to be adjusted according to experimental tests.

5. Cyclic strength reduction function

The *S-N* curves proposed in the previous section are fatigue life estimators for a material point with a fixed maximum stress and a given ratio *R*. If, after a number of cycles lower than the cycles to failure, the constant amplitude cyclic loads giving that maximum stress $S_{\max}$ (and ratio *R*) are removed, some change in S_u is expected due to accumulation of fatigue cycles. In order to describe the variation of S_u the following function is proposed:

$$\begin{aligned} fred(R, Ncycles) &= \exp(-B0 \cdot (\log 10(Ncycles))^{BETAF}) \\ B0 &= -\log 10(S_{\max} / S_u) / (\log 10(N_F))^{BETAF} \end{aligned} \tag{8}$$

BETAF is a material parameter and N_F the number of cycles to failure.

6. Time advancing strategy

An advantage of the methodology presented consists in the way the loading is applied. In a mechanical problem each load is applied in two intervals, in the following order (see Figure 3),

-**Tracing load**, (described by "ai" periods on Figure 3). It is used to obtain the stress ratio $R = S_{\min} / S_{\max}$ at each integration point, following the load path during several cycles until the R relationship tends to a constant value. This occurs when the following norm is satisfied,

$$\eta = \sum_{GP} \left\| \frac{R_{GP}^{i+1} - R_{GP}^{i}}{R_{GP}^{i+1}} \right\| \rightarrow 0 \qquad (9)$$

where $R_{GP}^{i} = S_{\min} / S_{\max} \big|_{GP}^{i}$ is computed at each Gauss interpolation point for the load increment "i".

-**Enveloping load**, (described by "bi" periods on Figure 3). After the first tracing load interval (ai), the number of cycles N is increased while keeping constant the maximum applied load (thick line in Figure 3) and the stress ratio R. In this new load interval, the variable is not the load level (kept constant) but the number of cycles.

This two-stages strategy allows a very fast advance in the time loading. A new interval with the two stages explained should be added for each change in the loading level.

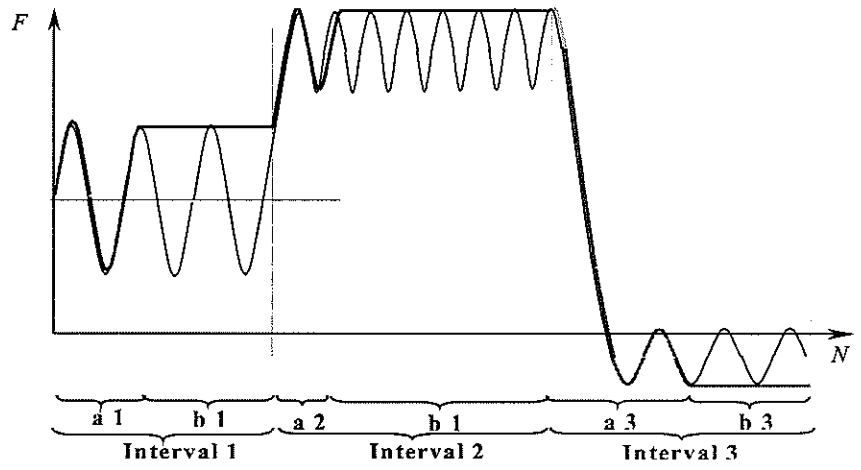

Figure 3. Schematic representation of the time advancing strategy

7. Numerical Application

A real industrial component, the aluminium alloy support of Fig. 1, was numerically analyzed to test the potential of the proposed formulation. This formulation has been implemented into a general-purpose thermo-mechanical finite element code (COMET, 00). The material strength is randomly assigned to each Gauss point using a normal distribution with mean value corresponding to porosity A2 material strength (see Section 2). Maximum and minimum values of material strength matching porosity A0 and A4, respectively. A *S-N* master curve, corresponding to experimental values for rotating bending fatigue of A2 material, was scaled down (or up) according to the randomly assigned material strength of each point. The results of fatigue damage localization obtained during different tests are summarized in Figure 4. The arrows show regions of damage different of the ones obtained previously with material characterized as homogenous and corresponding to experimental regions of failure (see Figure 1).

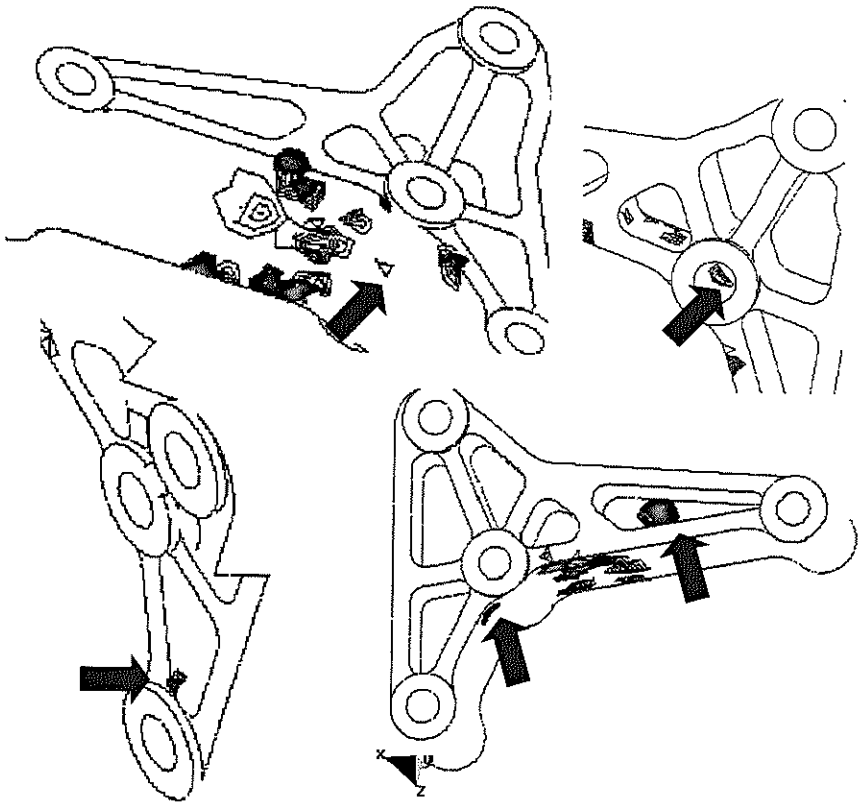

Figure 4. Fatigue damage localization obtained in different numerical analysis with a random material characterization.

8. Conclusions

A fatigue model based in continuum mechanics accounting for elasto-plastic-damage constitutive equations, previously developed by the authors, has been extended to include the influence of material internal defects. In this stress life approach the material is considered to be non-homogenous. The material strength is randomly assigned and Stress-N° of cycles curves are scaled down according to material strength of each point. Limit values for material strength are based on experimental tests of samples with different degree of porosity.

Preliminary results from the application of the formulation presented to the analysis of an aluminium industrial component, indicate that the approach is adequate for the fatigue analysis of metallic structures with scattered porosity and/or other internal defects.

Acknowledgements

The authors thank the financial support provided by European Commission under the CRAFT Project BES2-5637, DARCAST.. This support as well as the experimental results obtained by Politecnico de Torino on industrial components supplied by Fonderie 2A, Italy, are gratefully acknowledged.

9. References

Salomón O., Oller S., Oñate E., "Fatigue damage modelling and finite elements analysis methodology: Continuum basis and applications", to be presented at *FATIGUE 2002, 8th International Fatigue Congress*, Stockholm, Sweden, June 2002.

Oller S., Salomón O., Oñate E., "Thermo-mechanical fatigue analysis using generalized continuum damage mechanics and the finite element method", Sent for publication at: *Int. J. Numer. Meth. Engng*, 2001.

Salomón O., Oller S., Car E., Oñate E., "Thermo-mechanical fatigue analysis based on continuum mechanics", *Congreso Argentino de Mecánica Computacional, MECOM'99*, Mendoza, Argentina, 1999.

Suresh S., *Fatigue of Materials*, Cambridge Univ.Press, 2° edition, 1998.

Osgood C. *Fatigue Design*, Pergamon Press, 1982.

COMET Coupled Mechanics and Thermal Analysis. Data Input Manual. Technical Report N° 308, CIMNE, Barcelona, Jan 2000.

DARCAST Enhanced Design and Manufacturing of High Resistance Casted Parts. Final Technical Report. Craft Project N° : BES2-5637 funded by the European Community, Dec. 2000